Oxadiazon affects the expression and activity of aldehyde dehydrogenase and acylphosphatase in human striatal precursor

Title: Oxadiazon affects the expression and activity of aldehyde dehydrogenase and acylphosphatase in human striatal precursor cells: a possible role in neurotoxicity

Authors: Donatella Degl'Innocenti, Matteo Ramazzotti, Erica Sarchielli, Daniela Monti, Marta Chevanne, Gabriella Barbara Vannelli, Emanuela Barletta

PII: S0300-483X(18)30534-1
DOI: https://doi.org/10.1016/j.tox.2018.10.021
Reference: TOX 52122

To appear in: *Toxicology*

Received date: 26 June 2018
Revised date: 5 October 2018
Accepted date: 30 October 2018

Please cite this article as: Degl'Innocenti D, Ramazzotti M, Sarchielli E, Monti D, Chevanne M, Vannelli GB, Barletta E, Oxadiazon affects the expression and activity of aldehyde dehydrogenase and acylphosphatase in human striatal precursor cells: a possible role in neurotoxicity, *Toxicology* (2018), https://doi.org/10.1016/j.tox.2018.10.021

Oxadiazon affects the expression and activity of aldehyde dehydrogenase and acylphosphatase in human striatal precursor cells: a possible role in neurotoxicity

Donatella Degl'Innocenti [1,‡], Matteo Ramazzotti [1,‡], Erica Sarchielli [2], Daniela Monti [1], Marta Chevanne [3], Gabriella Barbara Vannelli [4], Emanuela Barletta [1*]

[1] Department of Experimental and Clinical Biomedical Sciences “Mario Serio", University of Florence, Florence, Italy.
[2] Department of Experimental and Clinical Medicine, University of Florence, Florence, Italy.
[3] Retired research fellow, Department of Experimental and Clinical Biomedical Sciences “Mario Serio", University of Florence, Florence, Italy.
[4] School of Human Health Sciences, University of Florence, Florence, Italy.
‡These authors contributed equally to this work.

***Corresponding author:** Emanuela Barletta
Department of Experimental and Clinical Biomedical Sciences “Mario Serio", Viale G.B. Morgagni 50 - 50134 Florence, Italy. e-mail: emanuela.barletta@unifi.it

Abstract

Exposure to herbicides can induce long-term chronic adverse effects such as respiratory diseases, malignancies and neurodegenerative diseases. Oxadiazon, a pre-emergence or early post-emergence herbicide, despite its low acute toxicity, may induce liver cancer and may exerts adverse effects on reproductive and on endocrine functions. Unlike other herbicides, there are no indications on neurotoxicity associated with long-term exposure to oxadiazon. Therefore, we have analyzed in primary neuronal precursor cells isolated from human striatal primordium (HSP) the effects of non-cytotoxic doses of oxadiazon on neuronal cell differentiation and migration, and on the expression and activity of the mitochondrial aldehyde dehydrogenase 2 (ALDH2) and of the acylphosphatase (ACYP). ALDH2 activity protects neurons against neurotoxicity induced by toxic aldehydes during oxidative stress and plays a role in neurodegenerative conditions such as Alzheimer's disease and Parkinson's disease. ACYP is involved in ion transport, cell differentiation, programmed cell death and cancer, and increased levels of ACYP have been revealed in fibroblasts from patients affected by Alzheimer's disease. In this study we demonstrated that non-cytotoxic doses of OXA were able to inhibit neuronal striatal cell migration and FGF2- and BDNF-dependent differentiation towards neuronal phenotype, and to inhibit the expression and activity of ALDH2 and to increase the expression and activity of ACYP2. In addition, we have provided evidence that in human primary neuronal precursor striatal cells the inhibitory effects of OXA on cell migration and differentiation towards neuronal phenotype were achieved through modulation of ACYP2. Taken together, our findings reveal for the first time that oxadiazon could exert neurotoxic effects by impairing differentiative capabilities of primary neuronal cells and indicate that ALDH2 and ACYP2 are relevant molecular targets for the neurotoxic effects of oxadiazon, suggesting a potential role of this herbicide in the onset of neurodegenerative diseases.

Abbreviations

OXA, oxadiazon [5-ter-butyl-3-(2,4-dichloro-5-isopropoxyphenyl)-l,3,4-oxadiazol-2(3H)-one]; ALDH, Aldehyde dehydrogenase; ALDH2, mitochondrial aldehyde dehydrogenase 2; ACYP, acylphosphatase; ACYP1, erythrocyte-type acylphosphatase 1; ACYP2, muscle-type acylphosphatase 2; HSP cells, human primary striatal precursor cells; pFN, human plasma fibronectin; GAP43, growth-associated protein 43; FGF2, basic fibroblast growth factor; BDNF brain-derived neurotrophic factor.

Keywords

Oxadiazon; neurotoxicity; neurodegenerative disease; ALDH2; ACYP

1. Introduction

Pesticides, a heterogeneous group of compounds, include herbicides, insecticides, fungicides, bactericides, disinfectants and animal repellents. Herbicides are one of the most used pesticides since they are massively employed in agriculture, in floriculture and in domestic gardening. Therefore, people living in geographical area where both agriculture and floriculture are the main source of occupation could be particularly exposed to the adverse effects of these compounds as contaminants of water, air and soil.

Exposure to pesticides may result in acute poisoning or can induce long-term chronic sub-lethal effects. Herbicides, especially the synthetic organic ones, have low acute toxicity for humans, because high levels of exposure are reached only if they are improperly used and disposed. A particular attention has been placed on the role of neurotoxicity of herbicides, such as dipyridyls herbicides and glyphosate-based herbicides (Cattani et al., 2017, 2014; Colle et al., 2018; Del Pino et al., 2017; Vaccari et al., 2017; Zhang et al., 2016), because, after cancer, the most frequent chronic diseases associated with long-term exposure to herbicides are neurodegenerative diseases (Costa et al., 2017; Mostafalou and Abdollahi, 2017; Sabarwal et al., 2018; Yan et al., 2016; Wang et al., 2016).

Oxadiazon (OXA), a member of the heterocyclic organic oxadiazole class of herbicides authorized in Europe (FR, IT, PT, SK), in U.S.A. (CA) and in Australia, is a widely used herbicide. OXA is characterized by low acute toxicity (Von Burg, 1994) and by a long persistence in the soil (Ambrosi et al., 1977; Barrett and Lavy, 1984). Although the main action of this herbicide is the inhibition of protoporphyrinogen oxidase (Matringe et al., 1989; Krijt et al., 1997, 1993), OXA has adverse effects on reproductive health and on endocrine function by inducing aromatase activity (Laville et al., 2006) and by activating pregnane X receptor (Lemaire et al., 2006). In addition, OXA can induce liver cancer by affecting the constitutive androstane receptor and peroxisome proliferator-activated receptor α (Kuwata et al., 2016; Richert et al., 1996). However, risk assessment of this herbicide conducted by the European Food Safety Authority (EFSA) in 2010 concluded that there

were no specific studies assessing OXA neurotoxicity (European Food Safety Authority, 2010). But even without specific experimental or clinical data, it could be reasonable to hypothesize that neurotoxicity of OXA falls in the so-called "silent neurotoxicity" (Kraft et al., 2016). In fact, adverse effects on the nervous system may remain clinically unapparent for a long latent period and only appropriate experimental protocols are able to unmask injuries which are not cytotoxic – i.e. not lethal - but can either induce cell vulnerability or loss of normal cell functions with subsequent additional insults (Costa, 2017).

In vitro models of neurodegenerative diseases, which employ primary neuronal cells, offer the advantage to allow investigation of the mechanisms of silent neurotoxicity by specific molecules or compounds (Schlachetzki et al., 2013).

Therefore in this study, we have analyzed the neurotoxic effects of OXA in a primary neuronal cell line isolated from human fetal striatal primordium which expresses both neuronal and striatal properties and is responsive to neurotrophins and growth factors (Sarchielli et al., 2014). In particular, we have evaluated the effects of non-cytotoxic doses of OXA on differentiation of HSP cells towards neuronal phenotype and on cell migration which are critical events in the establishment of proper neuronal connectivity and functioning. In addition, we have focused our attention on the effects of OXA on the expression of the mitochondrial aldehyde dehydrogenase 2 (ALDH2) and of acylphosphatase (ACYP) which have been associated with neurodegeneration (Grünblatt et al., 2016; Liguri et al., 1996).

Aldehyde dehydrogenase is a family of enzymes which catalyzes detoxification of aldehydes by oxidation of aldehydes to carboxylic acids including toxic metabolites of dopamine and of nor-epinephrine and epinephrine (Doorn et al., 2014). In the central nervous system impaired ALDH2 activity is related with neurodegeneration (Chen et al., 2016; Fitzmaurice et al., 2014; Ritz et al., 2016; Zhang et al., 2015).

Acylphosphatase (ACYP) is a family of cytosolic enzymes which hydrolyzes the carboxyl-phosphate bond in acylphosphates. Two isoforms of ACYP have been characterized, the

erythrocyte-type acylphosphatase 1 (ACYP1) and the muscle-type acylphosphatase 2 (ACYP2). Increased levels of ACYP have been revealed in fibroblasts isolated from patients affected by Alzheimer's disease (Liguri et al., 1996) and *in vitro* studies have documented a role of ACYP in differentiation of neuronal derivative cells (Cecchi et al., 2004) as well as other cell types (Chiarugi et al., 1997; Degl'Innocenti et al., 1999; Fiaschi et al., 2000). ACYP is further involved in several pathophysiological processes (Stefani et al., 1997) such as ion transport (Nediani et al., 2002; Tadini-Buoninsegni et al., 2003), programmed cell death (Degl'Innocenti et al., 2004; Giannoni et al., 2000) and cancer (Zhang et al., 2016).

This study aimed at evaluating the neurotoxicity of non-cytotoxic doses of oxadiazon, which might be especially relevant in populations exposed to environmental contamination by herbicides leading to increased risk to develop neurodegenerative diseases.

2. Materials and Methods

2.1 Herbicide

Oxadiazon [5-ter-butyl-3-(2,4-dichloro-5-isopropoxyphenyl)-l,3,4-oxadiazol-2(3H)-one] (OXA) was obtained from Sigma-Aldrich (CAS Number 19666-30-9; purity 99.9% by HPLC analysis). OXA was stored at -20°C in aliquots of stock solutions at a final concentration of 500 mM in DMSO. In order to prevent that the solvent DMSO could affect cell viability, OXA was diluted in the culture medium to the desired concentrations so that the final DMSO concentration did not exceeded 0.1% (v/v).

2.2 Cell line and culture conditions

Primary human striatal neuronal precursor cells (HSP cells), were isolated from fetal ganglionic eminence, the striatal primordium, as described previously (Sarchielli et al., 2014). HSP cells were composed of neural stem cells, neuronal-restricted progenitors and striatal neurons (Sarchielli et al., 2014). HSP cells were grown in Coon's modified Ham's F12 medium supplemented with 10% of heat-inactivated fetal bovine serum (FBS) (culture medium) in a 5% CO_2-humidified atmosphere at 37°C. Subconfluent monolayers were propagated using trypsin (0.025%) in EDTA (0.5 mM) and

primary cell cultures were maintained for 7-9 passages.

2.3 Cell viability assay

In order to identify the maximal dose of OXA that did not interfere with cell viability - i.e. without cytotoxic effects - a dose-response analysis was performed and viability of HSP cells was evaluated by trypan blue dye exclusion test, which identifies cells whose membrane is damaged, and by the 3-(4,5-dimethylthiazol-2-yl)-2,5-diphenyltetrazolium bromide (MTT) reduction assay, which identifies cells with impaired metabolic activity (Parimelazhagan, 2016; Adan, 2016).

In order to identify cell viability by trypan blue dye, cells detached by trypsinization from subconfluent cultures were seeded into 6-well plates at a density of 2 x 10^5 cells per well in the culture medium. After incubation for 24 hours at 37°C in a 5% CO_2-humidified atmosphere cells were exposed to serum-free medium supplemented with 250 μg/ml of heat-treated bovine serum albumin (adhesion medium) or to adhesion medium supplemented with 1:2 serially diluted doses of OXA ranging from 500 μM to 1.95 μM. After 24 hours of incubation at 37°C in a 5% CO_2-humidified atmosphere, cells were detached by trypsinization and resuspended in adhesion medium. Cell suspension was then diluted (1:1 dilution) with trypan blue solution (0.4% w/v, Sigma-Aldrich). Cells were then counted in a Bürker hemocytometer chamber. Viability was expressed as the percentage of live unstained cells relative to the number of total cells. The assay was performed in triplicate wells for each experimental condition.

In order to evaluate the reduction of MTT tetrazolium compound by viable cells, cells detached from subconfluent cultures were seeded into 96-well plates at a cell density of 10^5 cells per well in culture medium without phenol red. After incubation for 24 hours at 37°C in a 5% CO_2-humidified atmosphere, phenol free culture medium was removed, and cell monolayers were exposed to adhesion medium or to adhesion medium supplemented with 1:2 serially diluted doses of OXA as described above. After 24 hours of incubation at 37°C in a 5% CO_2-humidified atmosphere, cell viability was assayed accordingly to the Vybrant® MTT Cell Proliferation Assay protocol (Thermo Fisher Scientific, Inc.). The reduction of MTT tetrazolium compound by viable cells into the

colored formazan compound was determined by spectrophotometric reading at 570 nm wavelength. Cell viability was expressed as the percentage of absorbance of OXA-treated cells relative to unexposed control cells. The assay was performed in triplicate wells for each experimental condition.

2.4 Comet assay

The single cell gel electrophoresis (Comet assay) was performed to identify the maximal dose of OXA that did not induce genotoxic effects in HSP cells. For this purpose, the single cell gel electrophoresis was performed according to the OxiSelect™ Comet Assay Kit (3-Well Slides) protocol (Cell Biolabs, Inc.). Briefly, HSP cells were seeded into 100 mm cell culture dishes at a density of 2 x 10^6 cells per dish in culture medium. After 48 hours of incubation at 37°C in a 5% CO_2-humidified atmosphere, the culture medium was removed, and cell monolayers were exposed to adhesion medium or to adhesion medium supplemented with 1:2 serially diluted doses of OXA ranging from 500 µM to 1.95 µM. After incubation for 24 hours at 37°C in a 5% CO_2-humidified atmosphere, cells were detached and resuspended at a density of 1 x 10^5 cells/ml in ice cold phosphate buffered saline (PBS) without Mg^{2+} and Ca^{2+}. Cell suspension was then mixed with Comet Agarose at 1:10 ratio (v/v) and 75 µl aliquots were pipetted in each of well of OxiSelect™ Comet Slide in accordance with manufacturer's instructions. The slides, after incubation in freshly prepared chilled lysis buffer and in alkaline solution, were electrophoresed in a horizontal gel electrophoresis tank filled with freshly made alkaline electrophoresis buffer (1 mM Na_2EDTA and 300 mM NaOH, pH >13). After electrophoresis, the slides were dried and stained with the Vista Green DNA Dye (Cell Biolabs, Inc.). Slides were then examined using an epifluorescence microscope at 200x magnification. Fifty randomly selected cells per slide and duplicate slides for each experimental condition were analyzed using computer-assisted image analysis (CometScore™ Version 1.5, TriTek Corporation). Tail moment was chosen as an index of DNA damage since it considers both the tail length and the fraction of DNA in the comet tail (Tail moment = tail length x % of DNA in the tail).

Etoposide-treated Jurkat T Cells (OxiSelect™ Comet Assay Control Cells, Cell Biolabs, Inc.) were used as a positive DNA-damaged control in these tests. Etoposide-treatment always led to the expected increase in DNA migration and thus ensured the appropriate performance of the Comet assay.

2.5 Oxidative stress detection

In order to verify whether exposure of HSP cells to OXA leads to oxidative stress, intracellular reactive oxygen species (ROS) were first detected by the ROS assay kit with 2',7'-dichlorodihydrofluorescein diacetate (ab113851, DCFDA Cellular ROS Detection Assay Kit, Abcam). DCFDA is a fluorescent probe that can detect reactive oxygen species like hydrogen peroxide, peroxyl radical and peroxynitrite (Crow, 1997; Oparka et al., 2016; Seet et al., 2010) . After diffusion into cells, DCFDA is deacetylated by cellular esterases to the non-fluorescent DCF product which cannot diffuse out of cells. DCF is then oxidized by ROS in the fluorescent 2'-7'dichlorofluorescein (Wang and Joseph, 1999) which can be detected using fluorescence spectroscopy at 485 nm excitation and 535 nm emission wavelengths. Briefly HSP cells were seeded into 96-well plates coated with human plasma fibronectin (pFN) (20 µg/ml) at a cell density of 2.5 x 10^4 cells per well in serum-free adhesion medium without phenol red. After 24 hours of incubation at 37°C in a 5% CO_2-humidified atmosphere, cell monolayers were washed and incubated for 45 minutes at 37°C in the dark in the presence of 25 µM DCFDA diluted in serum-free adhesion medium without phenol red according to the manufacturer's instructions. Cells were then incubated for additional 1, 2, 3, 4, 6, 12, 24 hours with or without OXA (7.81 µM) according to the protocol. End-point fluorescence from triplicate wells for each experimental condition was measured in a fluorescence microplate reader (SpectraMax M2, Molecular Devices) at 485 nm excitation and 535 nm emission wavelengths.

Oxidative stress was further evaluated by the fluorogenic CellROX® green (Thermo Fisher Scientific, Inc.) which is able to detect superoxide anion and hydroxyl radical (Yang and Choi, 2018). CellROX® green in the reduced state is very weakly fluorescent, while upon oxidation

becomes fluorescent and binds to nuclear and mitochondrial DNA. Briefly, cells from subconfluent cultures were seeded into 96-well plates coated with human plasma fibronectin (pFN) (20 μg/ml) at a cell density of 2.5 x 10^4 cells per well in serum-free adhesion medium without phenol red or in serum-free adhesion medium without phenol supplemented with OXA (7.81 μM). After incubation for a period of 1, 2, 3, 4, 6, 12, 24 hours at 37°C in a 5% CO_2-humidified atmosphere, cell monolayers were exposed to CellROX® Green reagent (5 μM) according to the manufacturer's instructions. End-point fluorescence from triplicate wells for each experimental condition was measured in a fluorescence microplate reader (SpectraMax M2, Molecular Devices) at 485 nm excitation and 520 nm emission wavelengths.

2.6 Differentiation of HSP cells towards neuronal phenotype

Differentiation of HSP cells towards neuronal phenotype was tested by examining neurite extension and expression of the growth-associated protein 43 (GAP43) during exposure to basic fibroblast growth factor (FGF2) or to brain-derived neurotrophic factor (BDNF) as previously described (Sarchielli et al., 2014). Briefly, cells from subconfluent cultures were seeded at a density of 2.5 x 10^4 cells per cm^2 in 24-well plates coated with pFN (20 μg/ml) in the presence of adhesion medium or in adhesion medium supplemented with FGF2 (10 ng/ml), or with BDNF (50 ng/ml). In experiments performed to analyze the effect of OXA on differentiation towards neuronal phenotype, HSP cells were exposed to adhesion medium supplemented with OXA (7.81 μM), or with FGF2 (10 ng/ml) and OXA (7.81 μM), or with BDNF (50 ng/ml) and OXA (7.81 μM). After 24 hours of incubation at 37°C in a 5% CO_2-humidified atmosphere, cell monolayers were fixed with 2.5% glutaraldehyde in PBS and neurite extensions were examined by phase-contrast optics in ten randomly chosen fields from two replicate wells for each experimental condition. Cells were scored positive for neurite extension if processes were longer than one cell-body diameter.

In order to analyze protein expression of GAP43, HSP cells were seeded in 100 mm culture dishes coated with pFN (20 μg/ml) at a density of 5 x 10^6 cells per dish. Cell monolayers were then grown in a 5% CO_2-humidified atmosphere at 37°C in adhesion medium or adhesion medium

supplemented with FGF2, or with BDNF, or with OXA, or with FGF2 and OXA, or with BDNF and OXA as described above. After 24 hours of incubation, cells were collected and total proteins were extracted by RIPA lysis buffer supplemented with protease inhibitors (RIPA Lysis Buffer System, Santa Cruz Biotechnology, Inc.). Proteins were then determined by the method of Bradford (Bradford, 1976) and equal amounts of proteins (20 μg) were separated by SDS-PAGE and then transferred onto polyvinylidene difluoride (PVDF) membranes. Membranes, after blocking with 5% bovine serum albumin (BSA), were incubated overnight at 4°C with the primary anti-GAP43 antibody (1:500) (sc-7457, Santa Cruz Biotechnology, Inc.), or after stripping with the primary anti-β-actin antibody (1:10000) (sc-47778, Santa Cruz Biotechnology, Inc.). Membranes were then incubated with specific horseradish peroxidase-conjugated secondary anti-IgG antibodies. Bands were visualized using the enhanced chemiluminescence system (Pierce ECL Plus Substrate, Thermo Fisher Scientific, Inc.). The enhanced chemiluminescence signal was then captured on x-ray film (CL-XPosure Film, Thermo Fisher Scientific, Inc.) and images were digitally recorded using a 4800 dpi scanner in transmission mode (Epson Perfection V750 Pro, Seiko Epson Corporation). Protein bands were quantified using ImageJ 1.42 software (Schneider et al., 2012). Values of quantified bands were normalized against the housekeeping protein β-actin.

2.7 Evaluation of HSP cell motility

In order to evaluate the effect of exposure to OXA on HSP cell motility, it was performed the scratch wound healing assay by creating a gap (wound) in a confluent cell monolayer and then by capturing images of cells closing the gap at regular time intervals using time-lapse microscopy as previously described (Barletta et al., 2015). Briefly, HSP cells were seeded at high density (2×10^6 cells per dish) in 60 mm culture dishes in the presence of culture medium. After overnight incubation at 37°C in a 5% CO_2-humidified atmosphere, confluent cell monolayers were wounded with a sterile rounded glass tip and washed with PBS to discard detached cells. Cell monolayers were then incubated at 37°C in the presence of serum-free CO_2 independent medium (Gibco, Life Technology) supplemented with L-glutamine and with 250 μg/ml heat-treated BSA. In experiments

performed to analyze the effect of OXA on cell migration, HSP cells were exposed to serum-free CO_2 independent medium supplemented with heat-treated BSA and OXA (7.81 μM). The wounded cell-free area was then observed under phase contrast microscopy for 24 hours at 37°C and images from the same optical field were taken at regular time intervals using time-lapse microscopy. The gap distance (wound width) was then analyzed with the TScratch software (ETH CSElab, Zurich, Swiss). The gap distance of cell-free wounded area at time 0 hour was set as 100% and the gap distance of wounded area measured over the time was expressed as percentage of the original wounded area at time 0 hour. Data were reported as mean ± standard deviation of 5 consecutive frames taken every 1-minute interval.

2.8 Evaluation of ALDH2 and ACYP gene expression

The relative RNA expression level of ALDH2 and of ACYP in HSP cells was determined by real-time reverse transcription PCR. Briefly, HSP cells seeded in 100 mm culture dishes coated with pFN (20 μg/ml) were grown for 24 hours in a 5% CO_2-humidified atmosphere at 37°C in adhesion medium or in adhesion medium supplemented with OXA (7.81 μM). Cells were then detached and total RNA was extracted using the RNeasy Mini Kit protocol according to the manufacturer's instructions (Qiagen, Inc.). RNA concentration and purity was measured by considering absorbance at 260 nm and 280 nm. 1 μg of total RNA was then reversely transcribed using Superscript II reverse transcriptase kit (Invitrogen, Thermo Fisher Scientific, Inc.) according to manufacturer's instructions. Real-time PCR was performed as described (Barletta et al., 2015) using the following TaqMan Gene Expression Assays (Thermo Fisher Scientific, Inc.): ALDH2, Hs01007998_m1; erythrocyte-type acylphosphatase 1 (ACYP1), Hs00153847_m1; muscle-type acylphosphatase 2 (ACYP2), Hs01586472_m1; β-actin, Hs99999903_m1. Each reaction was performed in triplicate. Expression of β-actin was used as endogenous control, and quantification of relative expression was obtained by the comparative Ct method, $2^{-\Delta\Delta Ct}$**.** Data expressed as mean ± standard deviation were representative of three independent experiments with similar results.

2.9 Evaluation of ALDH2 and ACYP protein expression

In order to study the effect of exposure to OXA on protein expression of ALDH2 and ACYP, it was performed a near-infrared western blot analysis because it is more quantitative and suitable for simultaneous detection of several proteins than the enhanced chemiluminescence western blot analysis (Kondo et al., 2018; Mathews et al., 2015). HSP cells seeded in 100 mm culture dishes coated with pFN (20 μg/ml) at a density of 5 x 10^6 cells per dish were grown in the presence of adhesion medium or in adhesion medium supplemented with OXA (7.81 μM). After 24 hours of incubation at 37°C in a 5% CO_2-humidified atmosphere, total proteins from detached cells were extracted by RIPA lysis buffer and protein concentration was determined by the method of Bradford (Bradford, 1976) as described above. Equal amounts of total proteins (20 μg) were separated by 12% SDS-PAGE and then transferred onto PVDF membranes. Membranes, after blocking were exposed to the following primary antibodies: anti-ALDH2 antibody (1:200) (sc-48837, Santa Cruz Biotechnology, Inc.); anti-ACYP1 antibody (1:200) (sc-134246, Santa Cruz Biotechnology, Inc.); anti-ACYP2 antibody (1:100) (sc- 398251, Santa Cruz Biotechnology, Inc.). After an overnight incubation at 4°C with primary antibodies, membranes were washed and exposed to the following appropriate secondary near-infrared dye antibodies according to the manufacturer's instructions (LI-COR, Inc.): goat anti-mouse (1:15.000) (925-68070, LiCor IRDye 680RD, LI-COR, Inc.); goat anti-mouse IgG_1 (1:15.000) (926-32350, LiCor IRDye 800CW, LI-COR, Inc.); donkey anti-goat (1:15.000) (925-32214, LiCor IRDye 800CW, LI-COR, Inc.). The primary anti-β-actin antibody (1:10000) (sc-47778, Santa Cruz Biotechnology, Inc.) was used as a normalization antibody and revealed with the secondary goat anti-mouse antibody (1:15.000) (925-68070, LiCor IRDye 680RD, LI-COR, Inc.). Protein bands were then detected with near infrared fluorescence and digitally acquired (Li-Cor Odyssey 9120 Near Infrared Fluorescence Imager, LI-COR, Inc.). Bands from the digital images were quantified using ImageJ 1.42 software (Schneider et al., 2012).

2.10 Evaluation of ALDH2 and ACYP enzymatic activity

HSP cells seeded in 100 mm culture dishes coated with pFN (20 μg/ml) at a density of 5 x 10^6 cells per dish were grown in the presence of adhesion medium or in adhesion medium supplemented with

OXA (7.81 μM).

ALDH2 activity was determined spectrophotometrically by monitoring the reductive reaction of NAD^+ to NADH utilizing the Mitochondrial Aldehyde Dehydrogenase (ALDH2) Activity Assay Kit (ab115348, Abcam). Briefly, after 24 hours of incubation in the presence or in the absence of OXA (7.81 μM), cells were lysed and protein concentration was determined as described above. 100 μl aliquots of cell lysate diluted with incubation buffer (1:1) (protein range from 31.25 μg/ml to 750 μg/ml) were loaded into each well of a 96-well plates in triplicate and incubated for 3 hours at room temperature. At the end of incubation, cells were washed with wash buffer and 200 ml of activity solution were added to each well according to the manufacturer's instructions. The optical absorbance was then read on a microplate reader at a wavelength of 450 nm for 60 minutes at intervals of 20 seconds, and values were reported as mean ± standard deviation.

ACYP activity was stained after electrophoresis on a polyacrylamide gel according to the method by Mizuno et al. (Mizuno et al., 1989) because in total cell lysates might be present other phosphatases that could hydrolyze acylphosphates. Briefly, after 24 hours of incubation in the presence or in the absence of OXA (7.81 μM), cells were lysed as described above and equal amounts of total proteins (20 μg) were separated by 12% SDS-PAGE. After electrophoresis the gel was washed with deionized water and then incubated at room temperature in staining solution containing 32% (v/v) sodium acetate buffer (pH 5.3), 20% (v/v) 0.05 M acetyl phosphate, 80 mg/100ml $Pb(NO_3)_2$, 58% (v/v) H_2O_2. When white bands of lead phosphate became visible documenting ACYP activity (ACYP molecular weight about 11 kDa), staining was stopped by washing the gel with deionized water and by immersing the gel in 1% ammonium sulfite solution. The gel was then immersed in a solution containing 5% methanol and 7.5% acetic acid and then dried.

2.11 ACYP2 gene silencing

In order to inhibit ACYP2 gene expression, post-transcriptional gene silencing was obtained by the use of ACYP2 siRNA system (sc-38900, Santa Cruz Biotechnology, Inc.) according to the

manufacturer's instructions. For this purpose, we used a pool of 3 ACYP2-specific 19-25 nt small interfering RNA (siRNA) and a control siRNA, which consists of a scrambled sequence that does not lead to degradation of the specific mRNA. Briefly, HSP cells were seeded in 6-well plates at a density of 2 x 10^5 cells per well in culture medium. After 24 hours of growth (60% confluence), cultures were washed with serum-free siRNA transfection medium (Santa Cruz Biotechnology, Inc.). Cell monolayers were then transfected with 80 pmols siRNA diluted in transfection medium and grown for 7 hours at 37°C in a 5% CO_2-humidified atmosphere. Transfection medium was then replaced with normal culture medium and cells were incubated for an additional 18 hours. Transfected cells were then detached and assayed in the different experimental designs used in this study. The efficiency of gene silencing was evaluated by Western blotting analysis of ACYP2 protein expression. Protein bands were quantified using ImageJ 1.42 software (Schneider et al., 2012) and values of quantified bands were normalized against the housekeeping protein β-actin.

2.12 Evaluation of ACYP2 gene silencing on HSP neuronal differentiation and on cell migration during exposure to OXA

The effect of ACYP2 gene silencing on cell differentiation during exposure to OXA was analyzed in ACYP2 siRNA-transfected HSP cells by evaluating both the ability to extend neurites and the expression of the GAP43 protein. Briefly, HSP cells transfected with ACYP2 siRNA were seeded in 24-well plates coated with pFN (20 μg/ml) in the presence of adhesion medium supplemented with OXA (7.81 μM), or with OXA and FGF2 (10 ng/ml), or with OXA and BDNF (50 ng/ml). After 24 hours of incubation at 37°C in a 5% CO_2-humidified atmosphere, cell monolayers were fixed with glutaraldehyde and neurite extensions were examined by phase-contrast microscopy as described above.

GAP43 protein expression was analyzed by Western blotting. For this purpose, ACYP2 siRNA-transfected HSP cells were seeded in 100 mm culture dishes coated with pFN (20 μg/ml) at a density of 5 x 10^6 cells per dish. Cell monolayers were then grown in a 5% CO_2-humidified atmosphere at 37°C in adhesion medium supplemented with OXA, or with OXA and FGF2, or with

OXA and BDNF as described above. After 24 hours of incubation, total proteins were extracted by RIPA lysis buffer, separated by electrophoresis (equal amounts of proteins, 20 μg) and then transferred onto PVDF membranes. Membranes were incubated overnight with the primary anti-GAP43 antibody or, after stripping, with the primary anti-β-actin antibody and then incubated with specific horseradish peroxidase-conjugated secondary anti-IgG antibodies as described above. Bands were visualized by the enhanced chemiluminescence system. Protein bands were quantified using ImageJ 1.42 software (Schneider et al., 2012).

The effect of ACYP2 gene silencing on HSP cell migration was analyzed by the scratch wound healing assay as described above by creating a wound in a confluent cell monolayer of ACYP2 siRNA-transfected HSP cells. The wounded cell-free area was observed under phase contrast microscopy for 24 hours and images were taken at regular time intervals using time-lapse microscopy.

2.13 Statistical analysis

OriginPro 9.1 (OriginLab Corporation, MA, USA) was used for statistical analysis and data graphing. When not otherwise specified, data were expressed as mean ± standard deviation from 3 independent experiments. Differences between two groups – i.e. control compared to treatment-were analyzed by Student's *t* test where $p < 0.05$ was considered statistically significant. When more than two groups were compared, one-way or two-way analysis of variance (ANOVA) was used with post-hoc Tukey HSD test for corrected pairwise comparison. $p<0.05$ was considered statistically significant.

3. Results

3.1 Identification of non-cytotoxic dose of OXA

When compared to untreated control cells, both trypan blue dye exclusion test (Fig 1A), which identifies cells characterized by damaged membranes, and MTT reduction assay (Fig. 1B), which identifies cells characterized by cellular dysfunction, revealed that the viability of HSP cells exposed to increasing doses of OXA was more than 98% at doses in the range of 1.95 -7.81 μM.

Since 7.81 μM was the maximum dose of OXA corresponding to more than 98% of cell viability, this dose was assumed as the maximal non-cytotoxic dose - i.e. the highest dose that had no effect on cell viability-. Moreover, when HSP cells were exposed to 7.81 μM OXA, Comet assay revealed that Tail DNA was very low (Tail moment ≈ 0.1) and equal to control cells unexposed to OXA (Fig. 1C), indicating that 7.81 μM OXA had no genotoxic effects.

Furthermore, when HSP cells were exposed to 7.81 μM OXA in time course experiments within the 24 hours, neither DCFDA (Fig. 1D) nor CellROX® green (Fig. 1E) were able to detect any increment of fluorescent signal compared to unexposed control cells. These results indicate that exposure of HSP cells to 7.81 μM OXA was not able to induce production of ROS like hydrogen peroxide, peroxyl radical, peroxynitrite anion, superoxide anion and hydroxyl radical which are the main ROS detected by DCFDA and CellROX® green. We, therefore established that 7.81 μM OXA was a suitable dose to be used in all further experimental protocols of this study.

3.2 Effect of OXA on HSP cell differentiation towards neuronal phenotype

When HSP cells were induced to differentiate into neurons by the growth factor FGF2 or by the neurotrophin BDNF, there was an increase of percentage of neurite-bearing cells (≈ 50%) in comparison to unexposed control cells (≈ 25%) (Fig. 2A; Supplemental Fig. 1, cell images) and an increase in GAP43 protein expression a well known neuronal differentiation marker (Fig. 2B; Supplemental Fig.2, quantitation of band intensities). Stimulation of neuritogenesis and increase of GAP43 expression induced by FGF2 or BDNF were found to be reduced during exposure to OXA (Fig. 2A and 2B; Supplemental Fig. 1 and 2) suggesting that OXA inhibits neuronal differentiation of primary striatal precursor neuronal cells stimulated by growth factors and neurotrophins.

3.3 Effect of OXA on HSP cell motility

When HSP cell motility was evaluated by the scratch wound healing assay, we created a wound at time 0 and we measured the initial 100% cell-free area both in control cells and in cells exposed to OXA (Fig. 3A cell-free area = 100%; Fig. 3B time-lapse images). 24 hours after wounding, complete wound closure was observed in control cultures (Fig. 3A, cell-free area ≈ 1%; Fig. 3B

time-lapse image). After 24 hours exposure to OXA the cell-free area was about 50%, so the wound was far to be completely closed (Fig. 3A, cell-free area ≈ 50%; Fig. 3B, time-lapse images). These results indicate that exposure to OXA inhibits the migratory properties of primary neuronal precursor striatal cells.

3.4 Effect of OXA on expression and on the activity of ALDH2 and ACYP

The gene expression of ALDH2 and of the two isoenzymes of ACYP (erythrocyte-type ACYP1 and muscle-type ACYP2) was analyzed by real-time PCR. ALDH2 and ACYP2 genes were found to be expressed in HSP cells (Fig. 4A, Control). On the contrary, HSP cells did not express the ACYP1 gene (RT-PCR Ct values not detected, data not shown). In order to confirm these results, protein expression of ALDH2 and ACYP was then analyzed by Western blotting. As shown in Fig. 4, in untreated control HSP cells, an approximately 56.2 kDa protein band was identified by the anti-ALDH2 antibody (Fig. 4B and 4C), and an approximately 11 kDa protein band was identified by the anti-ACYP2 antibody (Fig. 4B). Anti-ACYP1 antibody failed to reveal a protein band of approximately 11 kDa (Fig. 4C). Since the erythrocyte-type ACYP1 was found to be not expressed either at gene and protein level, the effects of exposure to OXA on ACYP was evaluated for the isoenzyme ACYP2 only.

During exposure to OXA, both gene and protein expression of ALDH2 were significantly inhibited (Fig. 4A and 4B respectively), while both gene and protein expression of ACYP2 were increased (Fig. 4A and 4B, respectively). Western blot revealed that during exposure to OXA protein expression of ALDH2 was reduced by ≈ 2.5 fold in comparison to unexposed control HSP cells; while ACYP2 protein expression was increased by ≈ 2 fold (Fig. 4D).

To further confirm such results, the enzymatic activity of ALDH2 was tested by monitoring the reductive reaction of NAD^+ to NADH. Exposure to OXA reduced ALDH2 activity in HSP cells compared to cells in the control (Fig. 4E). On the contrary, ACYP2 activity was increased during exposure to OXA as revealed by staining the ACYP enzymatic product (Fig. 4F).

3.5 Effect of ACYP2 gene silencing on HSP cell differentiation and motility during exposure to

OXA

When the ACYP2 gene was silenced by specific siRNAs (Fig. 5A) expression of ACYP2 was almost totally inhibited (about 99% in comparison to the expression of control cells, Supplemental Fig. 3). Upon inhibition of ACYP2 gene by siRNA, exposure to OXA was no more able to exert an inhibitory effect on both neuritogenesis (Fig. 5B; Supplemental Fig. 1, cell images) and on GAP43 protein expression (Fig. 5C; Supplemental Fig. 4, quantitation of band intensities) stimulated by FGF2 or BDNF. Moreover, when motility of HSP cells transfected with ACYP2 siRNA was tested by the scratch wound healing assay, exposure to OXA failed to retard the closure of the wound, and cell-free area was quite completely closed after 24 hours as observed in control untransfected cells grown in absence of OXA (Fig. 6A, cell-free area ≈ 1%; Fig. 6B, time-lapse image). Taken together, these results indicate that ACYP2 gene silencing prevents the inhibitory effects of OXA on neuronal differentiation stimulated by growth factors and neurotrophins and on migration of primary striatal neuronal precursor cells.

4. Discussion

Neurotoxicity represents the second most common adverse effect after cancer related to chronic exposure to pesticides and herbicides (Cattani et al., 2014, 2017; Colle et al., 2018; Del Pino et al., 2017; Li et al., 2004; Mostafalou and Abdollahi, 2017; Vaccari et al., 2017; Zhang et al., 2016). Although oxadiazon is one of the most used herbicide across the world as pre- and post-emergence herbicide against annual grasses and broad-leaved weeds - in the United States, approximately 125 tons/20000 hectares of oxadiazon are applied annually (United States Environmental Protection Agency, 2003) - there are no specific epidemiological or experimental studies assessing oxadiazon neurotoxicity (European Food Safety Authority, 2010). The need to fill this lacuna inspired us to study oxadiazon neurotoxicity in an *in vitro* model of neuronal cells.

In a recent study by Fournier and colleague (Fournier et al., 2017) the relative neurotoxicity of semi-volatile organic compounds, including herbicides, was estimated by comparable benchmark concentrations based on neuronal death as a common end-point. However neurotoxicity could be

ascribed to modifications of several metabolic/signalling pathways that not necessarily directly lead to neuronal death but rather increase the susceptibility to others neurotoxic insults or alter normal functions with additional insults - i.e. the so-called “silent neurotoxic action” (Kraft et al., 2016). Therefore, the purpose of the present study was to identify morphological and biochemical targets of oxadiazon that could shed light on the role of this heterocyclic organic herbicide in the onset of neurodegenerations through a mechanism that resembles silent neurotoxicity. To this aim, we used a model of primary neural cells isolated from human fetal striatal primordium (Sarchielli et al., 2014) since impaired functions of striatal neurons are involved in neurodegenerative conditions such as Parkinson's disease and Huntington's disease (Florio et al., 2018; Morigaki and Goto, 2017; Pepeu and Giovannini, 2017) and grafts of striatal primordium in Huntington's patients reconstitute the striatum structure and reverse the disease symptoms (Gallina et al., 2014; Peschanski et al., 2004).

We first identified the non-cytotoxic dose of oxadiazon - i.e. the maximal dose that did not interfere with cell viability - which was in a micromolar range (7.81 µM) comparable to the non-cytotoxic doses that were also used in other *in vitro* studies on the metabolic effects of exposure to oxadiazon (Laville et al., 2006, Richert et al., 1996). Moreover, the dose of 7.81 µM was in the range of blood concentration that can be reached after absorption during the long-term exposure with a NOAEL of 0.36 mg/kg/day, the lowest NOAEL in rats (European Food Safety Authority, 2010; United States Environmental Protection Agency, 2003).

In our human primary striatal neuronal precursor cells, the maximal non-cytotoxic dose of oxadiazon was able to inhibit ALDH2 at levels of gene expression, protein expression and enzymatic activity. Mitochondrial ALDH2 is the most important enzyme in detoxification of aldehydes and thus it plays a pivotal role in reducing levels of such toxic aldehydes generated by ROS formation, especially in the brain (Chen et al., 2016). It has been revealed that α,β-unsaturated aldehydes, such as 4-hydroxynonenal, generated by ROS through lipid peroxidation, are involved in neurotoxicity associated with the pathogenesis of neurodegenerative diseases (Angelova and

Abramov, 2018; Xiao et al., 2017). Albeit in our neuronal cells the non-cytotoxic dose of oxadiazon did not directly induce any oxidative stress, as documented by the absence of detectable production of ROS and by the absence of DNA breaks which can be induced by many genotoxic agents including ROS, but oxadiazon might exert a silent neurotoxicity. In fact, due to the inhibition of the mitochondrial ALDH2, oxadiazon might be able to induce a higher susceptibility of neural cells to the toxic effects of ROS generated during other pathophysiological conditions or by others xenobiotics.

We have also revealed that oxadiazon at the maximal non-cytotoxic dose was able to inhibit stimulation of neuritogenesis and GAP43 expression by growth factors and neurotrophins and to impair cell migration of our striatal neuronal precursor cells. Common features of neurodegeneration are often inhibition of neuritogenesis, which prevents the ability to establish neural connections, and inhibition of migration of neural precursor, which prevents self-regenerative capabilities (Benitez-King et al., 2004; Compagnucci et al., 2016; Gangatharan et al., 2018; Kandasamy and Aigner, 2018; Veleri et al., 2018; Woodbury and Ikezu, 2014).

In the present study, we have provided evidence that cell functions related to maintenance of neuronal differentiation and plasticity were impaired by oxadiazon through modulation of ACYP2. Gene and protein expression and enzymatic activity of ACYP2 were increased by exposure to oxadiazon. Even more importantly, silencing of ACYP2 was able to abolish all the inhibitory effects of oxadiazon on neuronal differentiation and on cell migration. These results apparently contrast with a previous study which has revealed that in SH-SY5Y neuroblastoma cells transfected with ACYP2, as a green fluorescent fusion protein, overexpression of ACYP2 was able to induce neuritogenesis and GAP43 expression (Cecchi et al., 2004). However, it was also reported that in the same neuroblastoma SH-SY5Y cells, retinoic acid, a well known differentiating agent of neural progenitors (Reynolds et al., 2003; Zieger and Schubert, 2017), increased the expression of ACYP1 but not of ACYP2 (Pieri et al., 1997). In addition, it was reported that skin fibroblasts from donors affected by familial Alzheimer's disease expressed high levels of ACYP1 (Liguri et al., 1996). The

observed discrepancies between different studies may be explained by several factors concerning the different cell models and experimental procedures. Our human striatal neuronal precursor cells and fibroblasts obtained from donors represent normal human primary cells, while SH-SY5Y cells are a malignant neuroblastoma cell line which might not display all the true behaviours of normal neural cells. Indeed, it has been noticed that neuroblastoma cell lines might not be the best *in vitro* model to study neurotoxicity and therefore it should be preferred the use of primary neural precursor cells (Bal-Price et al., 2010; Breier et al., 2010; LePage et al., 2005). Moreover, although fluorescent fusion proteins represent a reliable tool to study several biological processes in living cells, conjugation of a protein with a fluorescent marker might have consequences on the functionality of the protein of interest (Guarino et al., 2018; Snapp, 2005).

In support of the role played by ACYP2 as a molecular target of neurotoxicity, there are recent studies which have revealed that polymorphisms in ACYP2 gene are associated with oxaliplatin-induced neurotoxicity and with altered telomere length/dysfunction (Cliff et al., 2017; Codd et al., 2013; Pooley et al., 2013; Terrazzino et al., 2015; Walsh et al., 2016; Won et al., 2012). Telomere length shortening has been associated with age-related neurodegenerative diseases (Cai et al., 2013) and their maintenance is essential to prolong stem cell function and to successfully enter in the neuronal differentiation program (Ferrón et al., 2009; Liu et al., 2018; Lobanova et al., 2017; Reichert and Stier, 2017).

5. Conclusions

This study for the first time has revealed that non-cytotoxic doses of oxadiazon induce neuronal dysfunction. Moreover, we found that the expression and activity of ALDH2 and ACYP2 represent important molecular targets of oxadiazon neurotoxicity. Oxadiazon neurotoxicity warns about the possibility that this herbicide, at low environmental chronic exposure, might concur with other toxicants to increase the risk for the general population to develop neurodegenerative diseases.

Conflict of interest

The authors declare that there are no conflicts of interest.

Acknowledgments

This work was supported by grant of Fondazione Cassa di Risparmio di Pistoia e Pescia (ID ROL 76, P.I. E.B.) and by grant of University of Florence (Fondi di Ateneo per la Ricerca Scientifica to D.D., D.M., M.C. and E.B.)

References

Adan A., Kiraz Y., Baran Y., 2016. Cell Proliferation and Cytotoxicity Assays. Curr. Pharm. Biotechnol. 17, 1213-1221. https://doi.org/10.2174/1389201017666160808160513.

Ambrosi D., Kearney P.C., Macchia J.A., 1977. Persistence and metabolism of oxadiazon in soils. J. Agric. Food Chem. 25, 868-872. https://doi.org/10.1021/jf60212a019.

Angelova P.R., Abramov A.Y., 2018. Role of mitochondrial ROS in the brain: from physiology to neurodegeneration. FEBS Lett. 592, 692-702. https://doi.org/10.1002/1873-3468.12964.

Bal-Price A.K., Hogberg H.T., Buzanska L., Coecke S., 2010. Relevance of in vitro neurotoxicity testing for regulatory requirements: challenges to be considered. Neurotoxicol. Teratol. 32, 36-41. https://doi.org/10.1016/j.ntt.2008.12.003.

Barletta E., Ramazzotti M., Fratianni F., Pessani D., Degl'Innocenti D., 2015. Hydrophilic extract from Posidonia oceanica inhibits activity and expression of gelatinases and prevents HT1080 human fibrosarcoma cell line invasion. Cell Adh. Migr. 9, 422-431. https://doi.org/10.1080/19336918.2015.1008330.

Barrett M.R., Lavy T.L., 1984. Effects of Soil Water Content on Oxadiazon Dissipation. Weed Science 32, 697-701. http://www.jstor.org/stable/4043992.

Benitez-King G., Ramírez-Rodríguez G., Ortíz L., Meza I., 2004. The neuronal cytoskeleton as a potential therapeutical target in neurodegenerative diseases and schizophrenia. Curr. Drug Targets CNS Neurol. Disord. 3, 515-533. https://doi.org/10.2174/1568007043336761.

Bradford M.M., 1976. A rapid and sensitive method for the quantitation of microgram quantities of protein utilizing the principle of protein-dye binding. Anal. Biochem. 72, 248-254. https://doi.org/10.1006/abio.1976.9999.

Breier J.M., Gassmann K., Kayser R., Stegeman H., De Groot D., Fritsche E., Shafer T.J., 2010. Neural progenitor cells as models for high-throughput screens of developmental neurotoxicity: state of the science. Neurotoxicol. Teratol. 32, 4-15. https://doi.org/10.1016/j.ntt.2009.06.005.

Cai Z., Yan L.J., Ratka A., 2013. Telomere shortening and Alzheimer's disease. Neuromolecular Med. 15, 25-48. https://doi.org/10.1007/s12017-012-8207-9.

Cattani D., Cesconetto P.A., Tavares M.K., Parisotto E.B., De Oliveira P.A., Rieg C.E.H., Leite M.C., Prediger R.D.S., Wendt N.C., Razzera G., Filho D.W., Zamoner A., 2017. Developmental exposure to glyphosate-based herbicide and depressive-like behavior in adult offspring: Implication of glutamate excitotoxicity and oxidative stress. Toxicology 387, 67-80. https://doi.org/10.1016/j.tox.2017.06.001.

Cattani D., de Liz Oliveira Cavalli V.L., Heinz Rieg C.E., Domingues J.T., Dal-Cim T., Tasca C.I., Mena Barreto Silva F.R., Zamoner A., 2014. Mechanisms underlying the neurotoxicity induced by glyphosate-based herbicide in immature rat hippocampus: involvement of glutamate excitotoxicity. Toxicology 320, 34-45. https://doi.org/10.1016/j.tox.2014.03.001.

Cecchi C., Liguri G., Fiorillo C., Bogani F., Gambassi M., Giannoni E., Cirri P., Baglioni S., Ramponi G., 2004. Acylphosphatase overexpression triggers SH-SY5Y differentiation towards neuronal phenotype. Cell. Mol. Life Sci. 61, 1775-1784. doi 10.1007/s00018-004-4192-y.

Chen C.H., Joshi A.U., Mochly-Rosen D., 2016. The Role of Mitochondrial Aldehyde Dehydrogenase 2 (ALDH2) in Neuropathology and Neurodegeneration. Acta Neurol. Taiwan 25, 111-123. http://www.ant-tnsjournal.com/Mag_Files/25-4/001.pdf

Chiarugi P., Degl'Innocenti D., Taddei L., Raugei G., Berti A., Rigacci S., Ramponi G., 1997. Acylphosphatase is involved in differentiation of K562 cells. Cell Death Differ. 4, 334-340. https://doi.org/10.1038/sj.cdd.4400230 .

Cliff J., Jorgensen A.L., Lord R., Azam F., Cossar L., Carr D.F., Pirmohamed M., 2017. The molecular genetics of chemotherapy-induced peripheral neuropathy: A systematic review and meta-analysis. Crit. Rev. Oncol. Hematol. 120, 127-140. https://doi.org/10.1016/j.critrevonc.2017.09.009.

Codd V., Nelson C.P., Albrecht E., Mangino M., Deelen J., Buxton J.L., Hottenga J.J., Fischer K., Esko T., Surakka I., Broer L., Nyholt D.R., Mateo Leach I., Salo P., Hägg S., Matthews M.K., Palmen J., Norata G.D., O'Reilly P.F., Saleheen D., Amin N., Balmforth A.J., et al., 2013.

Identification of seven loci affecting mean telomere length and their association with disease. Nat. Genet. 45, 422-427. https://doi.org/10.1038/ng.2528.

Colle D., Farina M., Ceccatelli S., Raciti M., 2018. Paraquat and Maneb Exposure Alters Rat Neural Stem Cell Proliferation by Inducing Oxidative Stress: New Insights on Pesticide-Induced Neurodevelopmental Toxicity. Neurotox. Res. (2018). https://doi.org/10.1007/s12640-018-9916-0.

Compagnucci C., Piemonte F., Sferra A., Piermarini E., Bertini E., 2016. The cytoskeletal arrangements necessary to neurogenesis. Oncotarget 7, 19414-1929. https://doi.org/10.18632/oncotarget.6838.

Costa C., Miozzi E., Teodoro M., Briguglio G., Rapisarda V., Fenga C., 2017. New insights on 'old' toxicants in occupational toxicology (Review). Mol. Med. Rep. 15, 3317-3322. https://doi.org/10.3892/mmr.2017.6374.

Costa L.G., 2017. Overview of Neurotoxicology. Curr. Protoc. Toxicol., 74, 11.1.1-11.1.11. https://doi.org/10.1002/cptx.36.

Crow J.P., 1997. Dichlorodihydrofluorescein and dihydrorhodamine 123 are sensitive indicators of peroxynitrite in vitro: implications for intracellular measurement of reactive nitrogen and oxygen species. Nitric Oxide 1, 145-157. https://doi.org/10.1006/niox.1996.0113.

Degl'Innocenti D., Marzocchini R., Malentacchi F., Ramazzotti M., Raugei G., Ramponi G., 2004. ACYP1 gene possesses two alternative splicing forms that induce apoptosis. IUBMB Life 56, 29-33. https://doi.org/10.1080/15216540310001654349.

Degl'Innocenti D., Marzocchini R., Rosati F., Cellini E., Raugei G., Ramponi G., 1999. Acylphosphatase expression during macrophage differentiation and activation of U-937 cell line. Biochimie 81, 1031-1035. doi 10.1016/S0300-9084(99)00333-8.

Del Pino J., Moyano P., Díaz G.G., Anadon M.J., Diaz M.J., García J.M., Lobo M., Pelayo A., Sola E., Frejo M.T., 2017. Primary hippocampal neuronal cell death induction after acute and repeated paraquat exposures mediated by AChE variants alteration and cholinergic and glutamatergic transmission disruption. Toxicology 390, 88-99. https://doi.org/10.1016/j.tox.2017.09.008.

Doorn J.A., Florang V.R., Schamp J.H., Vanle B.C., 2014. Aldehyde dehydrogenase inhibition generates a reactive dopamine metabolite autotoxic to dopamine neurons. Parkinsonism Relat. Disord. 20S1, S73-S75. https://doi.org/10.1016/S1353-8020(13)70019-1.

European Food Safety Authority, 2010. Conclusion on the peer review of the pesticide risk assessment of the active substance oxadiazone on request of EFSA. EFSA Journal 8, 1389. https://doi.org/10.2903/j.efsa.2010.1389.

Ferrón S.R., Marqués-Torrejón M.A., Mira H., Flores I., Taylor K., Blasco M.A., Fariñas I., 2009. Telomere shortening in neural stem cells disrupts neuronal differentiation and neuritogenesis. J. Neurosci. 29, 14394-14407. https://doi.org/10.1523/JNEUROSCI.3836-09.2009.

Fiaschi T., Chiarugi P., Veggi D., Raugei G., Ramponi G., 2000. The inhibitory effect of the 5' untranslated region of muscle acylphosphatase mRNA on protein expression is relieved during cell differentiation. FEBS Lett. 473, 42-46. https://doi.org/10.1016/S0014-5793(00)01496-4 .

Fitzmaurice A.G., Rhodes S.L., Cockburn M., Ritz B., Bronstein J.M., 2014. Aldehyde dehydrogenase variation enhances effect of pesticides associated with Parkinson disease. Neurology 82, 419-426. https://doi.org/10.1212/WNL.0000000000000083. Erratum in Neurology 83, 1879-1880. https://doi.org/10.1212/01.wnl.0000457072.94144.8f .

Florio T.M., Scarnati E., Rosa I., Di Censo D., Ranieri B., Cimini A., Galante A., Alecci M., 2018. The Basal Ganglia: More than just a switching device. CNS Neurosci. Ther. 24, 677-684. https://doi.org/10.1111/cns.12987.

Fournier K., Baumont E., Glorennec P., Bonvallot N., 2017. Relative toxicity for indoor semi volatile organic compounds based on neuronal death. Toxicol. Lett. 279, 33-42. https://doi.org/10.1016/j.toxlet.2017.07.875.

Gallina P., Paganini M., Biggeri A., Marini M., Romoli A., Sarchielli E., Berti V., Ghelli E., Guido C., Lombardini L., Mazzanti B., Simonelli P., Peri A., Maggi M., Porfirio B., Di Lorenzo N., Vannelli G.B., 2014. Human striatum remodelling after neurotransplantation in Huntington's disease. Stereotact. Funct. Neurosurg. 92, 211-217. https://doi.org/10.1159/000360583.

Gangatharan G., Schneider-Maunoury S., Breau M.A., 2018. Role of mechanical cues in shaping neuronal morphology and connectivity. Biol. Cell 110, 125-136. https://doi.org/10.1111/boc.201800003.

Giannoni E., Cirri P., Paoli P., Fiaschi T., Camici G., Manao G., Raugei G., Ramponi G., 2000. Acylphosphatase is a strong apoptosis inducer in HeLa cell line. Mol. Cell Biol. Res. Commun. 3, 264-270. https://doi.org/10.1006/mcbr.2000.0228 .

Grünblatt E., Riederer P., 2016. Aldehyde dehydrogenase (ALDH) in Alzheimer's and Parkinson's disease. J. Neural. Transm. 123, 83-90. https://doi.org/10.1007/s00702-014-1320-1.

Guarino A.M., Pollice A., Calabro V., 2018. GFP Fusion Proteins: A Solution or a Problem? Biomed. J. Sci. & Tech. Res. June 20. https://biomedres.us/pdfs/BJSTR.MS.ID.001258.pdf

Kandasamy M., Aigner L., 2018. Reactive Neuroblastosis in Huntington's Disease: A Putative Therapeutic Target for Striatal Regeneration in the Adult Brain. Front. Cell. Neurosci. 12, 37. https://doi.org/10.3389/fncel.2018.00037.

Kondo Y., Higa S., Iwasaki T., Matsumoto T., Maehara K., Harada A., Baba Y., Fujita M., Ohkawa Y., 2018. Sensitive detection of fluorescence in western blotting by merging images. PLoS One 13, e0191532. https://doi.org/10.1371/journal.pone.0191532.

Kraft A.D., Aschner M., Cory-Slechta D.A., Bilbo S.D., Caudle W.M., Makris S.L., 2016. Unmasking silent neurotoxicity following developmental exposure to environmental toxicants. Neurotoxicol. Teratol. 55, 38-44. https://doi.org/10.1016/j.ntt.2016.03.005.

Krijt J., Stranska P., Maruna P., Vokurka M., Sanitrak J., 1997. Herbicide-induced experimental variegate porphyria in mice: tissue porphyrinogen accumulation and response to porphyrogenic drugs. Can. J. Physiol. Pharmacol. 75, 1181-1187. https://doi.org/10.1139/y97-149.

Krijt J., van Holsteijn I., Hassing I., Vokurka M., Blaauboer B.J., 1993. Effect of diphenyl ether herbicides and oxadiazon on porphyrin biosynthesis in mouse liver, rat primary hepatocyte culture and HepG2 cells. Arch. Toxicol. 67, 255-261. https://doi.org/10.1007/BF01974344.

Kuwata K., Inoue K., Ichimura R., Takahashi M., Kodama Y., Yoshida M., 2016. Constitutive

active/androstane receptor, peroxisome proliferator-activated receptor α, and cytotoxicity are involved in oxadiazon-induced liver tumor development in mice. Food Chem. Toxicol. 88, 75-86. https://doi.org/10.1016/j.fct.2015.12.017.

Laville N., Balaguer P., Brion F., Hinfray N., Casellas C., Porcher J.M., Aït-Aïssa S., 2006. Modulation of aromatase activity and mRNA by various selected pesticides in the human choriocarcinoma JEG-3 cell line. Toxicology 228, 98-108. https://doi.org/10.1016/j.tox.2006.08.021.

Lemaire G., Mnif W., Pascussi J.M., Pillon A., Rabenoelina F., Fenet H., Gomez E., Casellas C., Nicolas J.C., Cavaillès V., Duchesne M.J., Balaguer P., 2006. Identification of new human pregnane X receptor ligands among pesticides using a stable reporter cell system. Toxicol. Sci. 91, 501-509. https://doi.org/10.1093/toxsci/kfj173.

LePage K.T., Dickey R.W., Gerwick W.H., Jester E.L., Murray T.F., 2005. On the use of neuro-2a neuroblastoma cells versus intact neurons in primary culture for neurotoxicity studies. Crit. Rev. Neurobiol. 17, 27-50. https://doi.org/10.1615/CritRevNeurobiol.v17.i1.20.

Li S., Crooks P.A., Wei X., de Leon J., 2004. Toxicity of dipyridyl compounds and related compounds. Crit. Rev. Toxicol. 34, 447-460. https://doi.org/10.1080/10408440490503143.

Liguri G., Cecchi C., Latorraca S., Pieri A., Sorbi S., Degl'Innocenti D., Ramponi G., 1996. Alteration of acylphosphatase levels in familial Alzheimer's disease fibroblasts with presenilin gene mutations. Neurosci. Lett. 210, 153-156. https://doi.org/10.1016/0304-3940(96)12696-3.

Liu M.Y., Nemes A., Zhou Q.G., 2018 The Emerging Roles for Telomerase in the Central Nervous System. Front. Mol. Neurosci. 11, 160. https://doi.org/10.3389/fnmol.2018.00160.

Lobanova A., She R., Pieraut S., Clapp C., Maximov A., Denchi E.L., 2017. Different requirements of functional telomeres in neural stem cells and terminally differentiated neurons. Genes Dev. 31, 639-647. https://doi.org/10.1101/gad.295402.116.

Mathews S.T., Graff E., Judd R.L., Kothari V., 2015. Comparison of Chemiluminescence vs. Infrared Techniques for Detection of Fetuin-A in Saliva. Methods Mol. Biol. 1314, 333-348.

https://doi.org/10.1007/978-1-4939-2718-0_34.

Matringe M., Camadro J.M., Labbe P., Scalla R., 1989. Protoporphyrinogen oxidase inhibition by three peroxidizing herbicides: oxadiazon, LS 82-556 and M&B 39279. FEBS Lett. 245, 35-38. https://doi.org/10.1016/0014-5793(89)80186-3.

Mizuno Y., Ohba Y., Fujita H., Kanesaka Y., Tamura T., Shiokawa H., 1989. Activity staining of acylphosphatase after gel electrophoresis. Anal. Biochem. 183, 46-49. https://doi.org/10.1016/0003-2697(89)90169-3.

Morigaki R., Goto S., 2017. Striatal Vulnerability in Huntington's Disease: Neuroprotection Versus Neurotoxicity. Brain Sci. 7, E63. https://doi.org/10.3390/brainsci7060063.

Mostafalou S., Abdollahi M., 2017. Pesticides: an update of human exposure and toxicity. Arch. Toxicol. 91, 549-599. https://doi.org/10.1007/s00204-016-1849-x.

Nediani C., Formigli L., Perna A.M., Pacini A., Ponziani V., Modesti P.A., Ibba-Manneschi L., Zecchi-Orlandini S., Fiorillo C., Cecchi C., Liguori P., Fratini G., Vanni S., Nassi P., 2002. Biochemical changes and their relationship with morphological and functional findings in pig heart subjected to lasting volume overload: a possible role of acylphosphatase in the regulation of sarcoplasmic reticulum calcium pump. Basic Res. Cardiol. 97, 469-478. https://doi.org/10.1007/s00395-002-0367-6.

Oparka M., Walczak J., Malinska D., van Oppen L.M.P.E., Szczepanowska J., Koopman W.J.H., Wieckowski M.R., 2016 Quantifying ROS levels using CM-H2DCFDA and HyPer. Methods 109, 3-11. https://doi.org/10.1016/j.ymeth.2016.06.008.

Parimelazhagan T., 2016. Determination of Cytotoxicity. Prog. Drug Res. 71, 159-161. https://doi.org/10.1007/978-3-319-26811-8_26.

Pepeu G., Giovannini M., 2017. The fate of the brain cholinergic neurons in neurodegenerative diseases. Brain Res. 1670, 173-184. https://doi.org/10.1016/j.brainres.2017.06.023.

Peschanski M., Bachoud-Lévi A.C., Hantraye P., 2004. Integrating fetal neural transplants into a therapeutic strategy: the example of H untington's disease. Brain 127, 1219-1228.

https://doi.org/10.1093/brain/awh145.

Pieri A., Liguri G., Cecchi C., Degl'Innocenti D., Nassi P., Ramponi G., 1997. Alteration of intracellular free calcium and acylphosphatase levels in differentiating SH-SY5Y neuroblastoma cells. Biochem. Mol. Biol. Int. 43, 633-641. https://doi.org/0.1080/15216549700204441.

Pooley K.A., Bojesen S.E., Weischer M., Nielsen S.F., Thompson D., Amin Al Olama A., Michailidou K., Tyrer J.P., Benlloch S., Brown J., Audley T., Luben R., Khaw K.T., Neal D.E., Hamdy F.C., Donovan J.L., Kote-Jarai Z., Baynes C., Shah M., Bolla M.K., Wang Q., Dennis J., et al., 2013. A genome-wide association scan (GWAS) for mean telomere length within the COGS project: identified loci show little association with hormone-related cancer risk. Hum. Mol. Genet. 22, 5056-5064. https://doi.org/10.1093/hmg/ddt355.

Reichert S., Stier A., 2017. Does oxidative stress shorten telomeres *in vivo*? A review. Biol. Lett. 13, 20170463. https://doi.org/10.1098/rsbl.2017.0463.

Reynolds C.P., Matthay K.K., Villablanca J.G., Maurer B.J., 2003. Retinoid therapy of high-risk neuroblastoma. Cancer Lett. 197, 185-192. https://doi.org/10.1016/S0304-3835(03)00108-3 .

Richert L., Price S., Chesne C., Maita K., Carmichael N., 1996. Comparison of the induction of hepatic peroxisome proliferation by the herbicide oxadiazon in vivo in rats, mice, and dogs and in vitro in rat and human hepatocytes. Toxicol. Appl. Pharmacol. 141, 35-43. https://doi.org/10.1016/S0041-008X(96)80006-8.

Ritz B.R., Paul K.C., Bronstein J.M., 2016. Of Pesticides and Men: a California Story of Genes and Environment in Parkinson's Disease. Curr. Environ. Health Rep. 3, 40-52. https://doi.org/10.1007/s40572-016-0083-2.

Sabarwal A., Kumar K., Singh R.P., 2018. Hazardous effects of chemical pesticides on human health-Cancer and other associated disorders. Environ. Toxicol. Pharmacol. 63, 103-114. https://doi.org/10.1016/j.etap.2018.08.018.

Sarchielli E., Marini M., Ambrosini S., Peri A., Mazzanti B., Pinzani P., Barletta E., Ballerini L., Paternostro F., Paganini M., Porfirio B., Morelli A., Gallina P., Vannelli G.B., 2014. Multifaceted

roles of BDNF and FGF2 in human striatal primordium development. An in vitro study. Exp. Neurol. 257, 130-147. https://doi.org/10.1016/j.expneurol.2014.04.021.

Schlachetzki J.C., Saliba S.W., Oliveira A.C., 2013. Studying neurodegenerative diseases in culture models. Rev. Bras. Psiquiatr. 35, S92-S100. https://doi.org/10.1590/1516-4446-2013-1159.

Schneider C.A., Rasband W.S., Eliceiri K.W., 2012. NIH Image to ImageJ: 25 years of image analysis. Nat. Methods 9, 671-675. https://doi.org/10.1038/nmeth.2089 .

Seet R.C., Lee C.Y., Lim E.C., Quek A.M., Huang S.H., Khoo C.M., Halliwell B., 2010. Markers of oxidative damage are not elevated in otherwise healthy individuals with the metabolic syndrome. Diabetes Care 33, 1140-1142. https://doi.org/10.2337/dc09-2124.

Snapp E., 2005. Design and use of fluorescent fusion proteins in cell biology. Curr. Protoc. Cell Biol. 27, 21.4.1-21.4.13. https://doi.org/10.1002/0471143030.cb2104s27.

Stefani M., Taddei N., Ramponi G., 1997. Insights into acylphosphatase structure and catalytic mechanism. Cell. Mol. Life Sci. 53, 141-151. https://doi.org/10.1007/PL00000585.

Tadini-Buoninsegni F., Nassi P., Nediani C., Dolfi A., Guidelli R., 2003. Investigation of Na(+),K(+)-ATPase on a solid supported membrane: the role of acylphosphatase on the ion transport mechanism. Biochim. Biophys. Acta 1611, 70-80. https://doi.org/10.1016/S0005-2736(02)00722-8.

Terrazzino S., Argyriou A.A., Cargnin S., Antonacopoulou A.G., Briani C., Bruna J., Velasco R., Alberti P., Campagnolo M., Lonardi S., Cortinovis D., Cazzaniga M., Santos C., Kalofonos H.P., Canonico P.L., Genazzani A.A., Cavaletti G., 2015. Genetic determinants of chronic oxaliplatin-induced peripheral neurotoxicity: a genome-wide study replication and meta-analysis. J. Peripher. Nerv. Syst. 20, 15-23. https://doi.org/10.1111/jns.12110.

United States Environmental Protection Agency, 2003. Reregistration Eligibility Decision (RED) for Oxadiazon. EPA 738-R-04-003. http://www3.epa.gov/pesticides/chem_search/reg_actions/reregistration/red_PC-109001_1-Sep-03.pdf.

Vaccari C., El Dib R., de Camargo J.L.V., 2017. Paraquat and Parkinson's disease: a systematic review protocol according to the OHAT approach for hazard identification. Syst. Rev. 6, 98. https://doi.org/10.1186/s13643-017-0491-x.

Veleri S., Punnakkal P., Dunbar G.L., Maiti P., 2018. Molecular Insights into the Roles of Rab Proteins in Intracellular Dynamics and Neurodegenerative Diseases. Neuromolecular Med. 20, 18-36. https://doi.org/10.1007/s12017-018-8479-9.

Von Burg R., 1994. Oxadiazon. J. Appl. Toxicol. 14, 69-71. https://doi.org/10.1002/jat.2550140113.

Walsh K.M., Whitehead T.P., de Smith A.J., Smirnov I.V., Park M., Endicott A.A., Francis S.S., Codd V., ENGAGE Consortium Telomere Group., Samani N.J., Metayer C., Wiemels J.L., 2016. Common genetic variants associated with telomere length confer risk for neuroblastoma and other childhood cancers. Carcinogenesis 37, 576-582. https://doi.org/10.1093/carcin/bgw037.

Wang H., Joseph J.A., 1999. Quantifying cellular oxidative stress by dichlorofluorescein assay using microplate reader. Free Radic. Biol. Med. 27, 612-616. https://doi.org/10.1016/S0891-5849(99)00107-0.

Wang M.D., Little J., Gomes J., Cashman N.R., Krewski D., 2016. Identification of risk factors associated with onset and progression of amyotrophic lateral sclerosis using systematic review and meta-analysis. Neurotoxicology 61, 101-130. https://doi.org/10.1016/j.neuro.2016.06.015.

Won H.H., Lee J., Park J.O., Park Y.S., Lim H.Y., Kang W.K., Kim J.W., Lee S.Y., Park S.H., 2012. Polymorphic markers associated with severe oxaliplatin-induced, chronic peripheral neuropathy in colon cancer patients. Cancer 118, 2828-2836. https://doi.org/10.1002/cncr.26614.

Woodbury M.E., Ikezu T.J., 2014. Fibroblast growth factor-2 signaling in neurogenesis and neurodegeneration. Neuroimmune Pharmacol. 9, 92-101. https://doi.org/10.1007/s11481-013-9501-5.

Xiao M., Zhong H., Xia L., Tao Y., Yin H., 2017. Pathophysiology of mitochondrial lipid oxidation: Role of 4-hydroxynonenal (4-HNE) and other bioactive lipids in mitochondria. Free Radic. Biol. Med. 111, 316-327. https://doi.org/10.1016/j.freeradbiomed..04.363.

Yan D., Zhang Y., Liu L., Yan H., 2016. Pesticide exposure and risk of Alzheimer's disease: a systematic review and meta-analysis. Sci. Rep. 6, 32222. https://doi.org/10.1038/srep32222.

Yang Z., Choi H., 2018. Single-Cell, Time-Lapse Reactive Oxygen Species Detection in E. coli. Curr. Protoc. Cell Biol. e60. https://doi.org/10.1002/cpcb.60.

Zhang F., Zhang Y., Deng Z., Xu P., Zhang X., Jin T., Liu Q., 2016. Genetic variants in theacylphosphatase 2 gene and the risk of breast cancer in a Han Chinese population. Oncotarget 7, 86704-86712. https://doi.org/10.18632/oncotarget.13495.

Zhang X., Ye Y.L., Wang Y.N., Liu F.F., Liu X.X., Hu B.L., Zou M., Zhu J.H., 2015. Aldehyde dehydrogenase 2 genetic variations may increase susceptibility to Parkinson's disease in Han Chinese population. Neurobiol. Aging 36, 2660.e9 - 2660.e13. https://doi.org/10.1016/j.neurobiolaging.2015.06.001.

Zhang X.F., Thompson M., Xu Y.H., 2016. Multifactorial theory applied to the neurotoxicity of paraquat and paraquat-induced mechanisms of developing Parkinson's disease. Lab. Invest. 96, 496-507. https://doi.org/10.1038/labinvest.2015.161.

Zieger E., Schubert M., 2017. New Insights Into the Roles of Retinoic Acid Signaling in Nervous System Development and the Establishment of Neurotransmitter Systems. Int. Rev. Cell Mol. Biol. 330, 1-84. https://doi.org/10.1016/bs.ircmb.2016.09.001.

Figure legends

Fig. 1. (A) Trypan blue dye exclusion test was used to evaluate HSP cell viability during exposure to OXA ranging from 1.95 μM to 500 μM. Values were expressed as the percentage of live unstained cells relative to the number of total cells and represent the mean ± standard deviation of 3 independent experiments. Data were compared by the one-way ANOVA with post-hoc Tukey HSD tests; * $p<0.05$ respect to unexposed control cells. (B) MTT assay was used to test cytotoxicity during exposure to OXA ranging from 1.95 μM to 500 μM. Values were expressed as the percentage of viable cells relative to viability of unexposed control cells and represent the mean ± standard deviation of 3 independent experiments. Data were compared by the one-way ANOVA with post-hoc Tukey HSD tests; * $p<0.05$ respect to unexposed control cells. (C) Genotoxicity evaluation of OXA by Comet assay. HSP cells were grown in absence (Control) or in presence of 7.81 μM OXA which was the maximum dose of OXA corresponding to more than 98% of cell viability. The tail moment was calculated as the product of the tail length and the fraction of total DNA in the tail. Values were expressed as mean ± standard deviation of fifty randomly selected cells from duplicate slides. Data of OXA exposed cells were compared with those measured in unexposed control cells by Student's t test. (D) ROS detection by DCFDA. Fluorescence in HSP cells grown in absence (Control) or in presence of 7.81 μM OXA was measured at the indicated time (485 nm excitation, 535 nm emission). Values were reported as mean ± standard deviation of 3 independent experiments. At different time points, data of OXA exposed cells were compared with those measured in unexposed control cells by Student's t test. (E) Quantification of ROS production by CellROX® Green Reagent. Fluorescence in HSP cells grown in absence (Control) or in presence of 7.81 μM OXA was measured at the indicated time (485 nm excitation, 520 nm emission). Values were reported as mean ± standard deviation of 3 independent experiments. At different time points, data of OXA exposed cells were compared with those measured in unexposed control cells by Student's t test.

Fig. 2. Effect of OXA on differentiation of HSP cells towards neuronal phenotype induced by FGF2 or BDNF. HSP cells were grown in absence (-) or in presence (+) of 10 ng/ml FGF2, 50 ng/ml BDNF, 7.81 μM OXA. (A) Neurite extension was examined by phase-contrast microscopy. Cells were scored positive for neurite extension if at least one neurite was longer than one cell-body diameter and the number of cells with neurites was expressed as the percentage of total cells in each microscopic field. Data are presented as mean ± standard deviation from ten microscopic fields from duplicate wells for each experimental condition. Representative images of cells are shown in Supplemental Fig. 1. Two-way ANOVA with post-hoc Tukey HSD tests were used for statistical analysis; * $p<0.05$ respect to unexposed control cells. (B) Representative enhanced chemiluminescent Western blot showing the results of different treatments on the expression of the neuronal growth cone marker GAP43. The housekeeping protein β-actin was used as an internal loading control. Values of quantified bands are shown in Supplemental Fig. 2.

Fig. 3. HSP cell migration was evaluated by the scratch wound assays. HSP cells were grown in absence (Control) or in presence of 7.81 μM OXA. After cells reached confluence, a gap or wound was created in the cell monolayer (time 0 hr) and images of cells closing the gap were taken every 1-minute interval for 24 hours. (A) Time course analysis of the wounded area in Control (hollow squares) or during exposure to OXA (black squares). For each experimental condition the gap distance at time 0 hr was set as 100% of wounded area and the width of wounded area measured over the time was expressed as the percentage of the original wounded area at time 0 hr. Data were reported as mean ± standard deviation of 5 consecutive frames taken every 1-minute interval. (B) Representative frames of wounded area at time 0 hr and after 24 hours of incubation in absence (Control) or in presence of 7.81 μM OXA.

Fig. 4. Expression of ALDH2 and ACYP in HSP cells grown in absence (Control) or in presence of 7.81 μM OXA. (A) Relative RNA expression of ALDH2 and of ACYP2 was detected by real-time reverse transcription. Expression of β-actin was used as endogenous control, and quantification of relative expression was obtained by the comparative Ct method, $2^{-\Delta\Delta Ct}$. Representative images of protein expression of ALDH2 and ACYP evaluated by near-infrared Western blot: (B) detection with primary anti-ALDH2 and anti-ACYP2 antibodies; (C) detection with anti-ALDH2 and anti-ACYP1; anti-β-actin antibody was used to detect β-actin as an housekeeping internal protein control (B, C). Molecular weight markers (MW), shown on the left of each panel B and C, are expressed in kilo Daltons (kDa). (D) Western blotting quantification of ACYP2 and ALDH2 protein expression normalized with respect to β-actin. (E) ALDH2 activity was detected spectrophotometrically in control cells (hollow squares) or in cells exposed to OXA (black squares) by monitoring the reductive reaction of NAD^+ to NADH in the protein range from 31.25 μg/ml to 750 μg/ml. The optical absorbance was read at 450 nm for 60 minutes at intervals of 20 seconds. (F) ACYP2 activity was detected by staining the enzyme activity after electrophoresis on a polyacrylamide gel according to the method by Mizuno and colleagues (Mitzuno et al., 1989) as described in Materials and Methods. White bands of lead phosphate became visible in correspondence of the molecular weight of ACYP (about 11 kDa).

Where indicated, values were reported as mean ± standard deviation of 3 independent experiments and results of OXA exposed cells were compared with those measured in untreated control cells by Student's t test; * $p<0.05$ was considered statistically significant.

Fig. 5. Effect of ACYP2 gene silencing on inhibition by OXA of FGF2- or BDNF-induced neuronal differentiation. ACYP2 gene expression in HSP cells was silenced by transfection with ACYP2-specific 19-25 nt small interfering RNA (siRNA). Control cells, siRNA (-), or cells transfected with ACYP2-siRNA, siRNA (+), were grown in the absence (-) or in presence (+) of 10 ng/ml FGF2, 50 ng/ml of BDNF, 7.81 μM OXA, as described in Materials and Methods. (A) Representative near-

infrared Western blot showing the efficiency of ACYP2 gene silencing by using anti-ACYP2 antibody; quantification of silencing efficiency is reported in Supplemental Fig. 3. (B) Evaluation of neurite extension was examined by phase-contrast microscopy and the number of cells with neurites was expressed as the percentage of the total cells in each microscopic field; representative images of cells are shown in Supplemental Fig. 1. Data are expressed as mean ± standard deviation from ten microscopic fields from two replicate wells for each experimental condition. Two-way ANOVA with post-hoc Tukey HSD tests were used for statistical analysis; * $p<0.05$ respect to unexposed control cells. (C) Representative Western blot images of GAP43 protein expression detected by enhanced chemiluminescence. The housekeeping protein β-actin was used as an internal loading control. Values of quantified bands are shown in Supplemental Fig. 4.

Fig. 6. Effect of ACYP2 gene silencing on inhibition by OXA of HSP cell motility. Cell migration was evaluated by the scratch wound assays as described in Materials and Methods. After cells reached confluence, a gap or wound was created in the cell monolayer (time 0 hr) and images of cells closing the gap were taken every 1-minute interval for 24 hours (24 hr). (A) Time course analysis of the wounded area in control (hollow squares) or in cells transfected with ACYP2-siRNA and exposed to OXA (7.81 μM) (black squares). Gap distance at time 0 hr was set as 100% and the width of wounded area measured over the time was expressed as the percentage of the original wounded area at time 0 hr. Data were reported as mean ± standard deviation of 5 consecutive frames taken every 1-minute interval. (B) Representative frames of wounded area at time 0 hr and

Fig 1

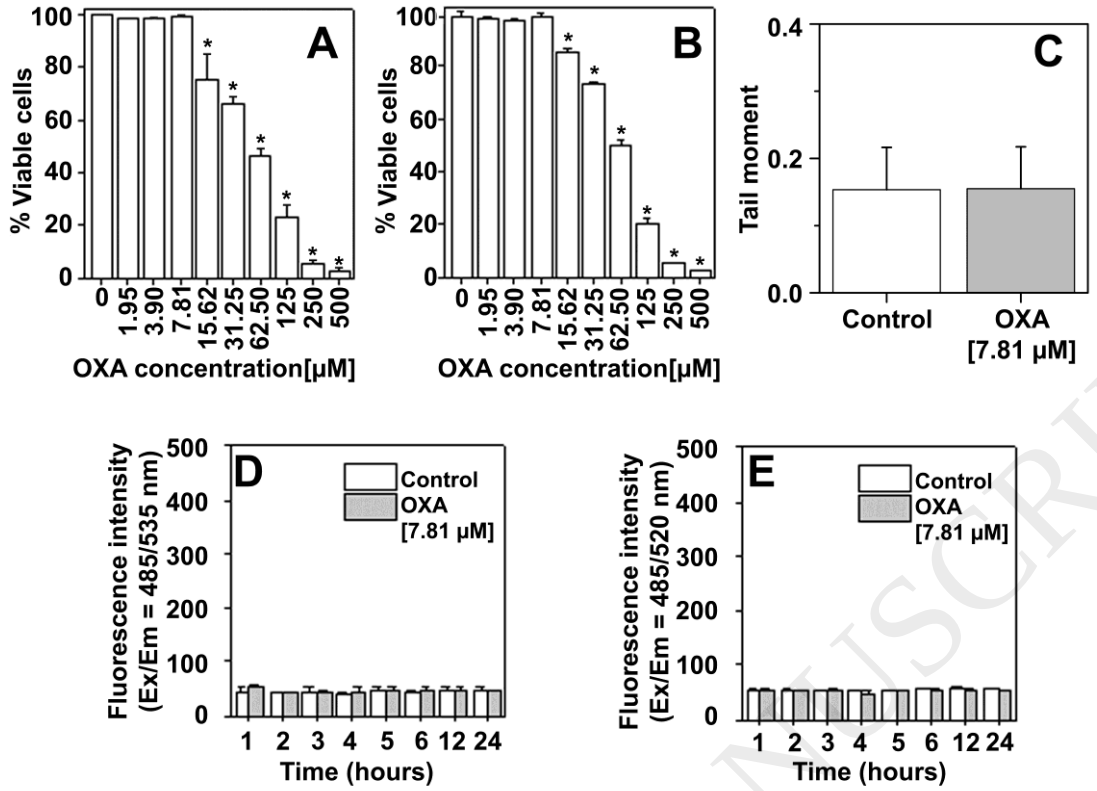

Fig 2

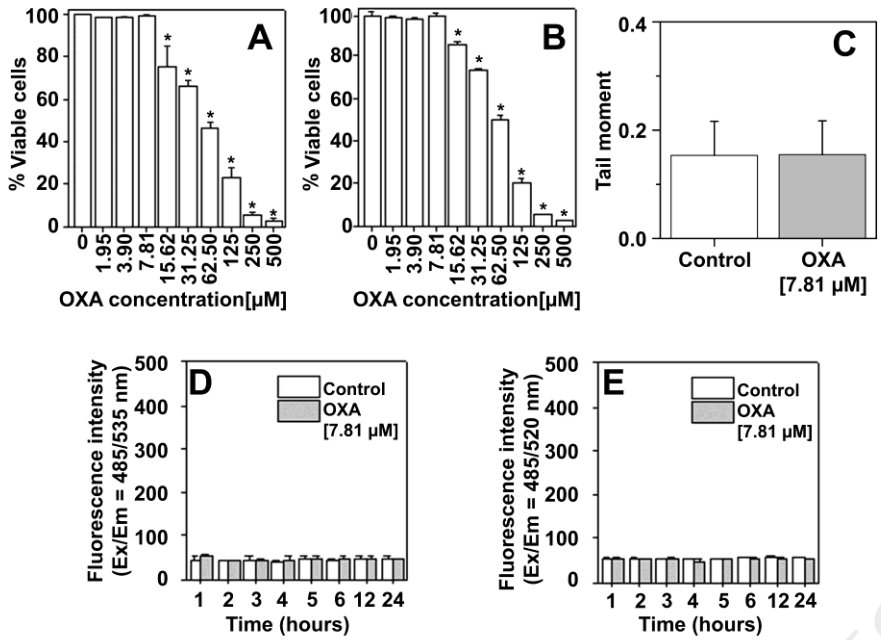

Fig 3

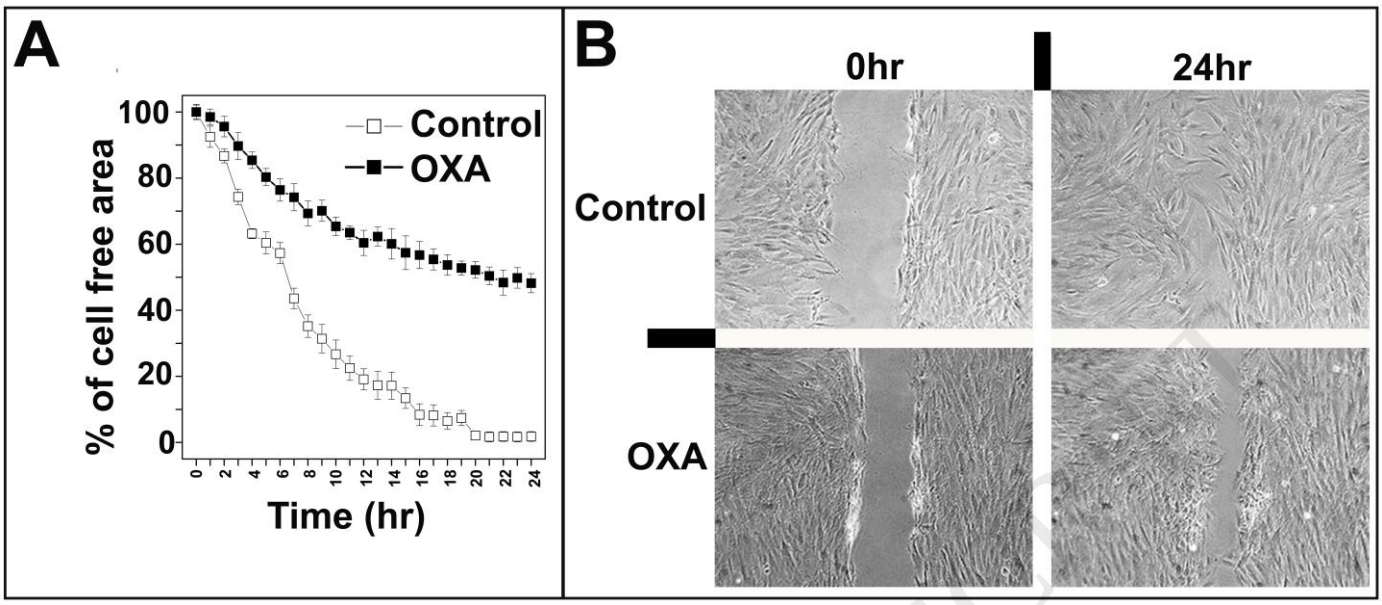

Fig 4

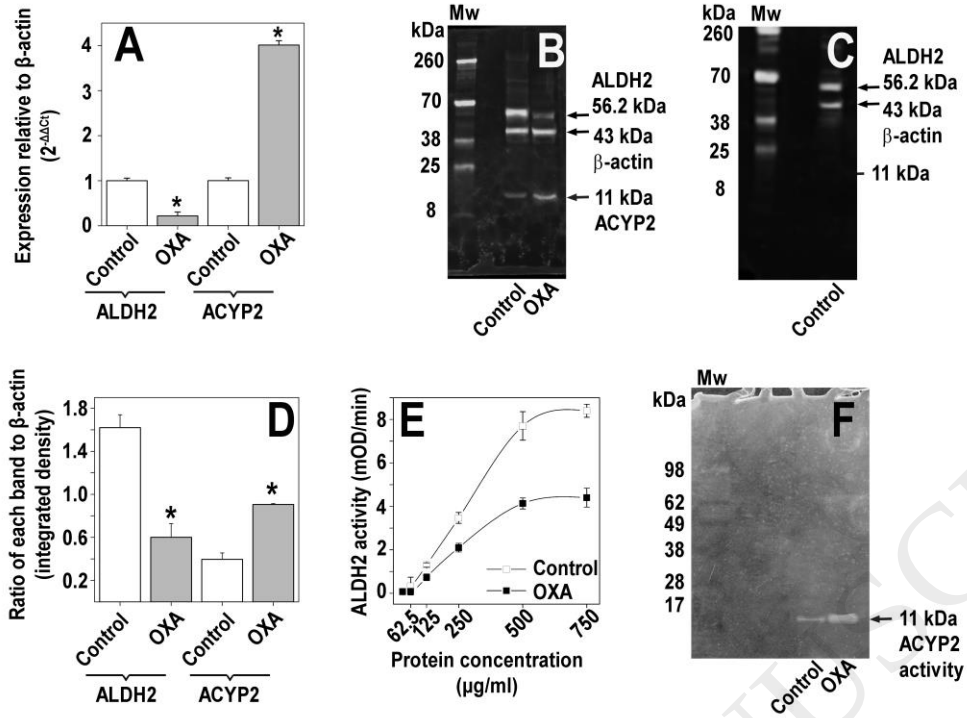

Fig 5

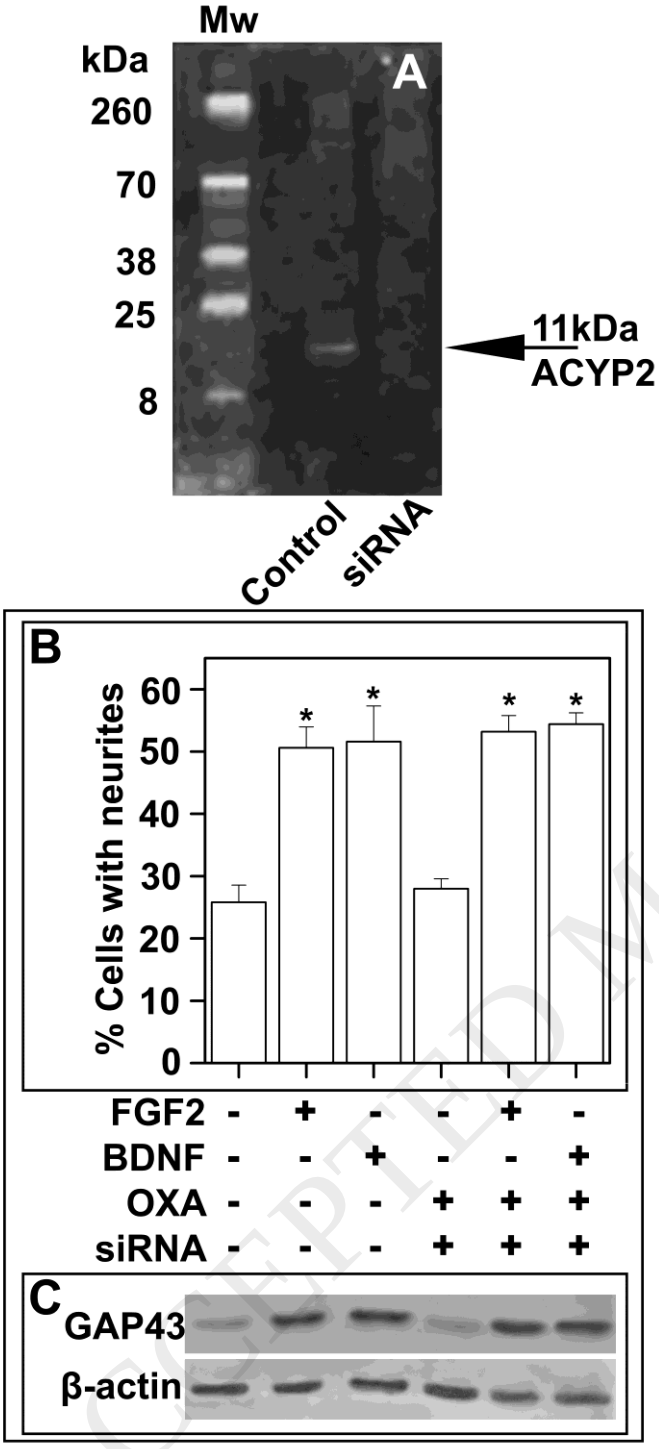

Fig 6